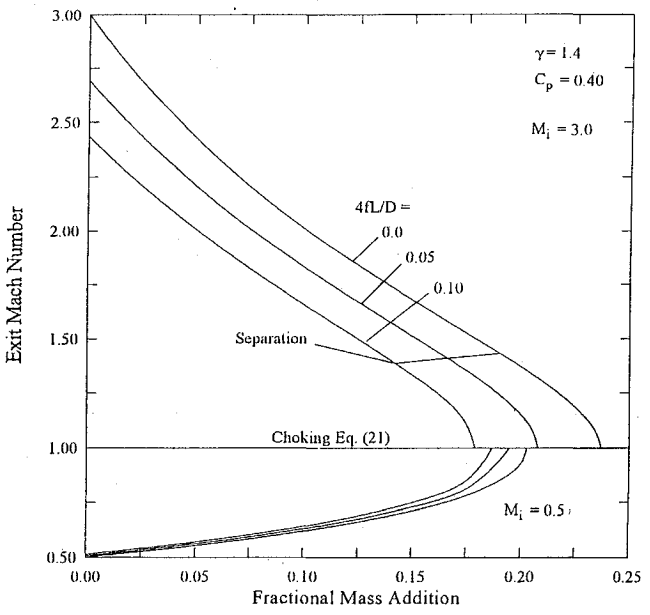

Fig. 3 Combined effects of mass addition and wall friction, $4f(L/D) = 0$ cases also appear in Fig. 1.

Most importantly, the information of Fig. 3 shows that wall friction should not have a dominant effect on the qualitative and quantitative behavior of the flow in typical experiments. The fractional mass addition for choking and separation is changed by less than 25% over the range of expected values of $4f(L/D)$.

Finally, the preceding equations Eq (24) may be combined with the definition of q to show that

$$\left(\frac{q_e}{q_i}\right)_s = 1 - \frac{C_p}{2} - 2f\frac{L}{D} \tag{25}$$

which leads to the conclusion that, regardless of the value of the inlet Mach number, q_e will always be at least about $0.8q_i$, and the average q, therefore, at least $0.9q_i$, thus supporting the earlier assertion that the local dynamic pressure does not vary much from inlet to exit.

Conclusions

This study has shown that there is a striking similarity between the influence of heat addition and mass addition on compressible flows. Most importantly, these results encourage the belief that relatively modest laboratory experiments employing mass addition can be devised that will reproduce the leading phenomena of heat addition, such as the axial variation of properties, choking, and wall boundary-layer separation. If so, the mass addition method could be further developed to explore and/or demonstrate the complex behavior of dual-mode ramjet/scramjet combustors.

Meanwhile, the insights into both types of flows found here further extend the already generous benefits of classical one-dimensional compressible flow analysis.

Acknowledgments

We are indebted to the U.S. Air Force Frank J. Seiler Research Laboratory for financial support and to the Department of Aeronautics of the U.S. Air Force Academy for its traditional hospitality and operational support of our work. The central concept for this research grew out of stimulating telephone discussions with Edward T. Curran, now Director of the Aero Propulsion and Power Directorate of the Wright Laboratory, that took place in 1992. His continuing interest in the project since then has also been of great value.

References

[1]Heiser, W. H., and Pratt, D. T., *Hypersonic Airbreathing Propulsion*, AIAA Education Series, Washington, DC, 1994, Chap. 6.

[2]Shapiro, A. H., *The Dynamics and Thermodynamics of Compressible Fluid Flow*, Ronald Press, New York, 1953, Chap. 8.

[3]Keuthe, A. M., and Chow, C. Y., *Foundations of Aerodynamics*, John Wiley, New York, 1986, pp. 413–418.

Effect of Ambient Turbulence Intensity on Sphere Wakes at Intermediate Reynolds Numbers

J.-S. Wu* and G. M. Faeth†
University of Michigan, Ann Arbor, Michigan 48109

Nomenclature

C_d	= drag coefficient
d	= sphere diameter, m
ℓ	= characteristic wake width, Eq. (2), m
Re, Re_t	= sphere and turbulence Reynolds numbers, $d\bar{U}_\infty/\nu$ and $d\bar{U}_\infty/\nu_t$
r	= radial position, m
$\bar{U}_t$	= wake-scaling velocity, Eq. (2), m/s
$\bar{U}_\infty$	= mean relative velocity of sphere, m/s
$\bar{u}$, $\bar{u}'$	= mean and rms fluctuating streamwise velocities, m/s
$\bar{v}'$	= rms fluctuating cross-stream velocity, m/s
x	= streamwise distance from center of sphere, m
ν, ν_t	= molecular and turbulence kinematic viscosities, m^2/s

Subscripts

c	= centerline value
o	= virtual origin condition
∞	= ambient condition

Introduction

RECENT studies of turbulence generation in dispersed multiphase flows have motivated the need for more information about the structure of sphere wakes at intermediate Reynolds numbers[1] ($10 < Re < 1000$), prompting earlier measurements of sphere wakes in nonturbulent environments[2] and in turbulent environments having an ambient turbulence intensity of 4.0% (Refs. 3 and 4). The observations of sphere wakes in turbulent environments indicated that whereas the wakes were turbulent, their mean streamwise velocities scaled like self-preserving laminar wakes with constant but enhanced viscosities due to the presence of the turbulence.[3] Thus, based on classical similarity analysis of self-preserving round laminar wakes with constant viscosities, the mean streamwise velocities in the wakes could be scaled as follows[3,5,6]:

$$\bar{u}/\bar{U}_t = [d/(x - x_o)]\exp(-r^2/2\ell^2) \tag{1}$$

where the wake-scaling velocity and characteristic wake width are

$$\bar{U}_t/\bar{U}_\infty = C_d\, Re_t/32, \qquad \ell/d = [2(x - x_o)/d\, Re_t]^{\frac{1}{2}} \tag{2}$$

and the effective turbulence viscosity appears in Re_t. Effective turbulence viscosities were relatively independent of position and the ratios of integral and Kolmogorov length scales to d (for the ranges 11–59 and 0.08–0.80, respectively); nevertheless, they increased with Re and exhibited low and high Re regimes separated by a transition regime where effects of vortex shedding were prominent in

Received June 27, 1994; revision received Aug. 25, 1994; accepted for publication Sept. 3, 1994.

*Postdoctoral Research Fellow, Department of Aerospace Engineering, 3000 FXB Building. Member AIAA.

†Professor, Department of Aerospace Engineering, 3000 FXB Building. Fellow AIAA.

power spectra measured in the near-wake region ($300 \leq Re \leq 600$). Unfortunately, the effect of ambient turbulence intensity on the existence and properties of laminar-like turbulent wakes was not resolved in Ref. 3; therefore, the objective of the present investigation was to resolve effects of ambient turbulence intensity variations on sphere wakes at intermediate Re.

Experimental Methods

The sphere wakes were observed within regions having relatively constant turbulence intensities using low- and high-turbulence wind tunnels having length scales similar to Ref. 3. The test arrangement for the high-turbulence wind tunnel was the same as Ref. 3, except that a perforated disk was centered on the duct axis near its downstream end, yielding a slowly decaying turbulence field so that sphere wakes could be observed at turbulence intensities of 7.0 and 9.5%, with mean and fluctuating ambient velocities varying less than 1% over the region of interest. The turbulence in the low-turbulence wind tunnel was generated by a perforated disk, followed by a nozzle contraction, yielding an ambient turbulence intensity of 2.0% with mean and fluctuating velocities varying less than 1% over the region of interest. Other aspects of the experiments—the properties and mounting of the test spheres, the laser velocimeters (LV) to measure ambient and wake flow properties, and experimental uncertainties—all were identical to Ref. 3, and a complete summary of test conditions and data can be found in Ref. 4.

Results and Discussion

Vortex Shedding

The effect of Re on vortex shedding was similar to the findings of Ref. 3 over the present range of turbulence intensities: effects of vortex shedding could only be observed in the temporal power spectra for Re in the range 300–600 for turbulence intensities $\leq$7.0%; and effects of vortex shedding were no longer apparent in the temporal power specta at higher turbulence intensities.

Mean Velocities

Typical measurements of mean streamwise velocities are illustrated in Fig. 1. Similar to findings at all ambient turbulence intensities considered, three wake regions are observed: a near-wake region, a laminar-like turbulent wake region, and a final decay region. The laminar-like turbulent wake region is the most prominent of the three, with mean streamwise velocities scaling according to Eq. (1). The near-wake region [for $(x - x_o)/d < 2$] exhibits effects of vortex shedding for Re in the range 300–600, similar to the observations of Ref. 3. The final decay region [for $(x - x_o)/d > 40$] is characterized by conditions where the mean streamwise velocity defect of the wake is comparable to the ambient turbulent fluctuations; this region exhibits a faster decay rate of mean streamwise velocities than any other axisymmetric wake region observed thus far.[2–4]

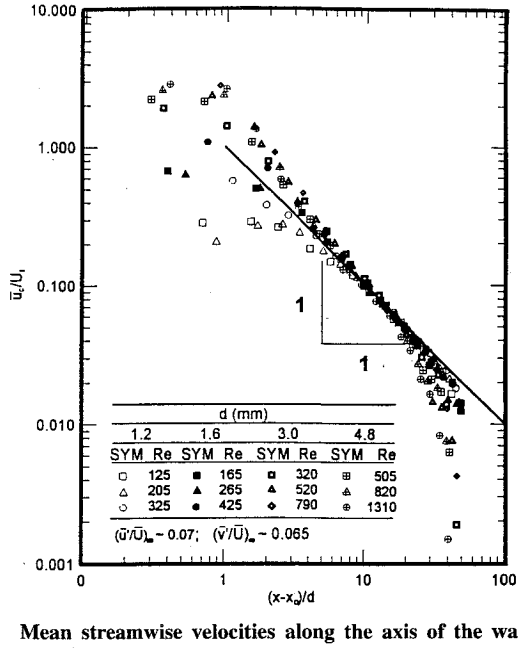

Fig. 1 Mean streamwise velocities along the axis of the wakes for $(\bar{u}'/\bar{U})_\infty$ = 7.0%.

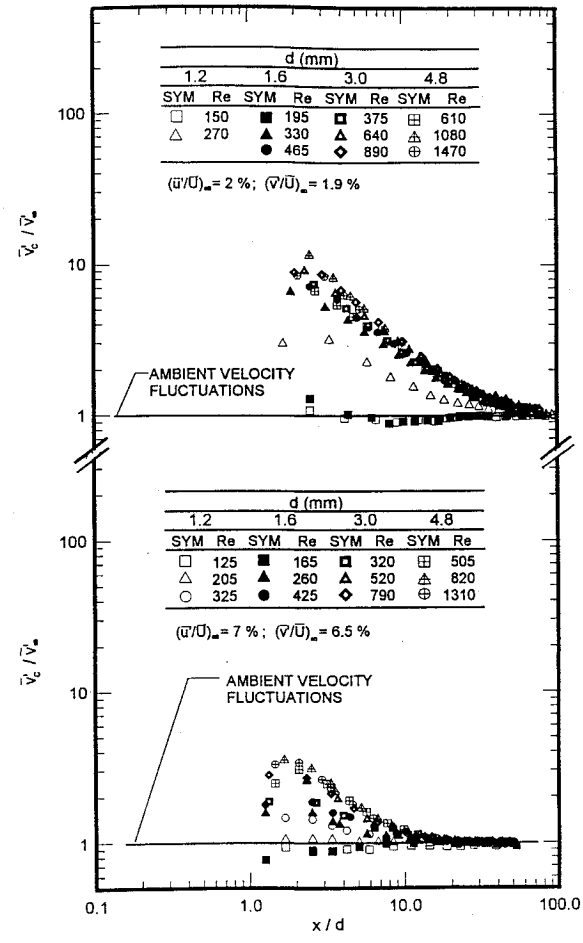

Fig. 2 Cross-stream velocity fluctuations along the axis of the wakes for $(\bar{u}'/\bar{U})_\infty$ = 2.0 and 7.0%.

Velocity Fluctuations

Effects of vortex shedding, wake turbulence, and ambient turbulence on effective turbulent viscosities for the laminar-like turbulent wake region are best illustrated by cross-stream velocity fluctuations; therefore, a sample of these results is illustrated in Fig. 2. Similar to the temporal power spectra of cross-stream velocity fluctuations,[4] the results illustrated in Fig. 2 can be separated into three regimes: 1) prior to the onset of vortex shedding ($Re < 300$), the velocity fluctuations in the wake are relatively small, comparable to the ambient velocity fluctuations; 2) when effects of vortex shedding are observed in near-wake temporal spectra ($300 < Re < 600$), the cross-stream velocity fluctuations progressively increase with increasing Re; and 3) at high Re($Re > 600$), where effects of vortex shedding are no longer observed in the near-wake temporal spectra, $\bar{v}_c'/\bar{v}_\infty'$ become independent of Re. In the high Re regime, values of $\bar{v}_c'$ are substantially enhanced from ambient turbulence levels near the start of the laminar-like turbulent wake region, but they progressively decrease and reach ambient turbulence levels at the start of the final decay region.

Effective Turbulence Viscosity

The value of the effective turbulent viscosity ν_t was found similar to Ref. 3. As noted earlier, ν_t is relatively independent of position within the laminar-like turbulent wake region but it varies as both Re and $(\bar{u}'/\bar{U})_\infty$ are varied, as illustrated in Fig. 3. Similar to the other turbulence properties of laminar-like turbulent wakes, it is evident that ν_t exhibits low, transition, and high Re regimes associated with vortex shedding behavior. The variation of ν_t/ν with Re is nearly

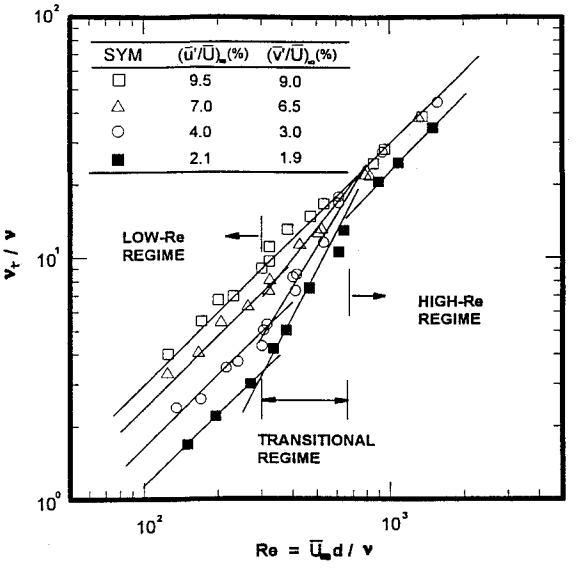

Fig. 3 Variation of turbulence viscosity with sphere Reynolds number and ambient turbulence intensity.

linear for a particular value of $(\bar{u}'/\bar{U})_\infty$ in the low Re range, with values progressively increasing as $(\bar{u}'/\bar{U})_\infty$ increases. This behavior can be explained based on crude mixing-length concepts of turbulent transport, e.g., $\nu_t - \nu \sim \bar{v}'\ell$. Now $\bar{v}' \sim \bar{v}'_\infty$ before vortex shedding begins whereas $\ell \sim d$ since the sphere size tends to control the width of the flow in the critical region near the start of the laminar-like turbulent wake. Thus, $\nu_t - \nu \sim \bar{v}'d \approx (\bar{v}'/\bar{U})_\infty \bar{U}_\infty d$ or $\nu_t/\nu - 1 \sim Re(\bar{v}'/\bar{U})_\infty$. This implies that ν_t/ν should increase linearly with both increasing Re and $(\bar{v}'/\bar{U})_\infty \sim (\bar{u}'/\bar{U})_\infty$, similar to the behavior observed in Fig. 3.

The variation of ν_t/ν also is nearly linear in Re in the high Re regime but is less dependent on the ambient turbulence intensity. This behavior can be explained by invoking the same mixing-length argument as before although noting that $\nu_t \gg \nu$ in the high Re regime. Then, $\nu_t/\nu \sim \bar{v}'\ell/\nu$ and in the laminar-like turbulent wake, $\bar{v}' \sim \bar{U}_\infty \gg \bar{v}'_\infty$. Estimating $\ell \sim d$, as before, then yields $\nu_t/\nu \sim \bar{U}_\infty d/\nu = Re$, generally, as observed in Fig. 3. As a result, ν_t/ν mainly is independent of $(\bar{v}'/\bar{U})_\infty \sim (\bar{u}'/\bar{U})_\infty$ in this high Re regime although the presence of ambient turbulence is needed to initiate laminar-like turbulent wake behavior. Finally, for an ambient turbulence intensity of 9.5%, effects of vortex shedding are suppressed due to the high-turbulence levels, as discussed earlier, so that high Re behavior persists to the smallest Re considered. Whether this behavior is representative of all higher ambient turbulence levels, as suggested by behavior in the high Re regime, is an interesting issue that should be resolved.

The rate of increase of ν_t/ν with increasing Re is more rapid in the transition regime than in the other two regimes [except when $(\bar{u}'/\bar{U})_\infty = 9.5\%$ which was just discussed]. Properties of ν_t/ν are most complex in this regime since its limits at low and high Re must accommodate rather different responses to variations of ambient turbulence intensities.

Conclusions

The present study considered sphere wakes for $Re = 125$–1560, $(\bar{u}'/\bar{U})_\infty = 2.0$–$9.5\%$, and ratios of the ambient integral and Kolmogorov length scales to d in the ranges 8–59 and 0.05–1.08, respectively. The major conclusions are as follows. 1) The wakes were turbulent but scaled like self-preserving laminar wakes with enhanced viscosities due to the presence of turbulence. 2) The effective turbulent viscosities were relatively independent of position and ratios of ambient integral and Kolmogorov length scales to d, however, they varied with both Re and $(\bar{u}'/\bar{U})_\infty$ in a low Reynolds number regime ($Re < 300$) and with Re alone in a high Reynolds number regime ($Re > 600$), with the transition regime between them associated with significant effects of vortex shedding from the sphere. 3) The laminar-like turbulent wake region was followed by a final decay region beginning when $\bar{u}_c \sim \bar{u}'_\infty$, which exhibits faster decay rates than any other axisymmetric wake observed thus far.

Acknowledgments

This research was sponsored by the Air Force Office of Scientific Research, Air Force Systems Command, USAF, under Grant F49620-92-J-0399.

References

[1]Mizukami, M., Parthasarathy, R. N., and Faeth, G. M., "Particle-Generated Turbulence in Homogeneous Dilute Dispersed Flows," *International Journal of Multiphase Flow*, Vol. 18, No. 3, 1992, pp. 397–412.

[2]Wu, J.-S., and Faeth, G. M., "Sphere Wakes in Still Surroundings at Intermediate Reynolds Numbers," *AIAA Journal*, Vol. 31, No. 8, 1993, pp. 1448–1455.

[3]Wu, J.-S., and Faeth, G. M., "Sphere Wakes at Moderate Reynolds Numbers in a Turbulent Environment," *AIAA Journal*, Vol. 32, No. 3, 1993, pp. 535–541.

[4]Wu, J.-S., "The Structure of Sphere Wakes at Intermediate Reynolds Numbers in Still and Turbulent Environments," Ph.D. Thesis, Department of Aerospace Engineering, Univ. of Michigan, Ann Arbor, MI, 1994.

[5]Tennekes, H., and Lumley, J. L., *A First Course in Turbulence*, Massachusetts Inst. of Technology Press, Cambridge, MA, 1972, pp. 113–124.

[6]Schlichting, H., *Boundary Layer Theory*, 7th ed., McGraw-Hill, New York, 1977, pp. 234–235 and 599.

Hypersonic Shock-Induced Combustion in a Hydrogen-Air System

J. K. Ahuja* and S. N. Tiwari†
Old Dominion University, Norfolk, Virginia 23529
and
D. J. Singh‡
Analytical Services and Materials, Inc., Hampton, Virginia 23666

Introduction

FOR an efficient propulsion system at hypersonic speeds, the combustion must take place at supersonic speeds. One of the proposed modes of propulsion is the shock-induced combustion ramjet (shramjet) in which a shock is employed to increase the temperature of premixed fuel and air to a point where chemical reaction will start. Apparent advantages of the shramjet over the scramjet engine include very short-length combustors and simple engine geometries. The phenomena of shock induced combustion/detonation around bodies traveling at hypersonic speeds is of great theoretical interest because of the need to understand the basic mechanism of combustion instabilities.

In the past, many researchers have conducted ballistic range experiments to study supersonic combustion/detonation. In these experiments, projectiles were fired in different premixed fuel air mixtures, and detonation structures around the projectiles were recorded. Every gas mixture has a detonation wave velocity known as Chapman-Jouget (C-J) velocity, which is characteristic of the mixture. If the velocity of the projectile is above the C-J velocity of the reactive mixture, the freestream velocity is referred to as overdriven. On the other hand, if the projectile velocity is lower than the C-J velocity, the freestream velocity is referred to as underdriven. For a given projectile diameter, the detonation wave structure is

Received Nov. 27, 1993; revision received April 12, 1994; accepted for publication Aug. 10, 1994.

*Graduate Research Assistant, Department of Mechanical Engineering. Student Member AIAA.

†Eminent Professor, Department of Mechanical Engineering. Associate Fellow AIAA.

‡Senior Research Scientist. Member AIAA.